Earth Systems and Environment (2023) 7:649–659
https://doi.org/10.1007/s41748-023-00348-y

ORIGINAL ARTICLE

Urbanisation and Geographical Signatures in Observed Air Temperature Station Trends Over the Mediterranean and the Middle East–North Africa

Panos Hadjinicolaou[1] · **Anna Tzyrkalli**[1] · **George Zittis**[1] · **Jos Lelieveld**[1,2]

Received: 2 November 2022 / Revised: 3 April 2023 / Accepted: 31 May 2023 / Published online: 1 July 2023

Abstract
We update observed temperature trends in the Mediterranean and the Middle East–North Africa (MENA) region, assess their temporal and spatial features and investigate possible influences from urbanisation. Monthly mean temperature time-series of 370 stations are acquired from the CRUTEM4.6 and GSOD datasets and converted into suitable format for statistical analysis. The calculated annual and seasonal temperature linear trends for 1981–2020 indicate a strong warming with a MENA station average annual trend equal to 0.36°C/decade and a faster warming rate for spring (0.43°C/decade) and summer (0.45°C/decade). These trends are correlated with longitude, revealing faster warming rates over the eastern Mediterranean and Middle East. The stations are characterised as rural or urban centre with the use of the Global Human Settlement Model (GHS-SMOD) spatial grid that accounts for population, city size and shape for the year 2000. The trend derived for the urban centre stations is an annually averaged 0.1°C/decade greater than for the rural or all stations, and more prominent during summer and autumn. Hence a discernible, but small, urbanisation signature is revealed.

Keywords Temperature trends · MENA region · Station data · Urbanisation

1 Introduction

According to recent calculations based on observational datasets, reiterated in the Intergovernmental Panel on Climate Change (IPCC) Sixth Assessment Report (AR6) Chapter 2, the globally averaged land surface air temperature in 2011–2020 was higher by 1.6°C relative to 1851–1900 (Gulev et al. 2021). In the region encompassing the Middle East North Africa (MENA) and the Mediterranean, mean and extreme temperatures have increased faster than the global average and rainfall has decreased considerably in recent decades (Lelieveld et al. 2012; Zittis 2018; Ntoumos et al. 2020), as also reported in the IPCC AR6 Chapter 10 on the links between global and regional climate change (Doblas-Reyes et al. 2021). For example, Almazroui et al. (2013a) calculated an overall warming rate of 0.6°C/decade in annual temperature during 1978–2010 for the majority of analysed stations around Saudi Arabia, which is 3 times larger than the reported global average (Hansen et al. 2010). Climate model projections indicate even warmer and drier conditions for the rest of the 21st century due to continuing anthropogenic climate forcing (Almazroui 2019; Zittis and Hadjinicolaou 2017; Zittis et al. 2019; Driouech et al. 2020). The analysis by Zittis et al. (2019) of multi-model regional climate simulations reveals a year-round warming by the end of the century of up to 5°C with respect to a 1986–2005 reference period. This warming is projected to be strongest during summer (up to 7°C), while the inferred rainfall reduction (between 10% and 40%) is not statistically robust. The observed increasing rate of heat extremes and the further projected warming raise concerns about the human comfort and survivability across the MENA (Lelieveld et al. 2016) and particularly the Middle East (Almazroui 2020) that justify frequent updates of the temperature evolution in the region.

✉ Jos Lelieveld
jos.lelieveld@mpic.de

Panos Hadjinicolaou
p.hadjinicolaou@cyi.ac.cy

[1] Atmosphere and Climate Research Centre (CARE-C), The Cyprus Institute, 2121 Nicosia, Cyprus

[2] Department of Atmospheric Chemistry, Max Plank Institute for Chemistry, 55020 Mainz, Germany

Long-term assessments of observed temperature change over extended land areas are typically made using gridded datasets based on monthly mean time-series from meteorological station measurements (Hansen et al. 2010; Jones et al. 2012; Rohde et al. 2013; Yun et al. 2019; Osborn et al. 2020) or global re-analyses (Simmons et al. 2017). For the Mediterranean and the Middle East, Tanarhte et al. (2012), in the only region-wide observationally based assessment utilising several datasets, derived warming rates between 0.2 – 0.4°C/decade in the annual mean temperature for 1961–2000 over most of the sub-regions analysed. The results differed among the inter-compared datasets due to the limited number of stations in the MENA and the influence of the schemes used to interpolate the sparse data. Such structural uncertainty of the gridded temperature datasets, also comprises land station homogenisation uncertainty, sensor exposure, errors arising from incomplete measurement sampling within grid-boxes, and bias related uncertainties arising from urbanisation (Morice et al. 2012), as also discussed in the IPCC AR6 Chapter 10 (Doblas-Reyes et al. 2021). These uncertainties can be quantified by elaborated error models (Brohan et al. 2006) and provide the datasets with an ensembles range (Morice et al. 2012) to complement global and hemispheric average temperature assessments (Jones 2016).

One of the above biases, the urbanisation effect due to the Urban Heat Island (UHI) phenomenon (Oke 1982) is noteworthy in rapidly urbanising regions, as it adds to the large-scale warming due to global climate change (He et al. 2013; Jones et al. 2008), but estimation of this urban warming is uncertain (Wang and Yan 2016). For China, Sun et al. (2016) applied an optimal fingerprinting analysis based on observed urban-rural station differences and estimated that, for the period 1961–2013, the warming attributed to urbanisation was 0.49°C (or 0.09°C/decade), about a third of the total temperature increase of 1.44°C. However, Wang et al. (2015), by incorporating the proportions of urban and rural areas for the stations considered, found that the spatially weighted urban and rural temperature averages reduce the estimated urban effects to less than 1%. Kalnay et al. (2006) found with an "observation minus reanalysis" difference method that a trend of 0.09°C/decade of mean temperature over eastern United States is due to land processes including urbanisation. It has been also recently highlighted in the IPCC AR6 Chapter 10 (Box 10.3 Urban climate processes and trends) that although observed warming trends in the cities can be partly attributed to urbanisation, they have negligible effect on the global annual mean surface air temperature (Doblas-Reyes et al. 2021).

The total population of the MENA region has increased fivefold since the 1950s, from just under 110 million in 1950 to 569 million in 2017 and absolute population numbers are expected to further double to over 1 billion inhabitants by 2100, according to medium variant projections (Mckee et al. 2017). There is no evidence that this remarkable demographic trend and the associated urbanisation have an impact on the air temperature trends in the region. Almazroui et al. (2013b), in the only relevant study for the MENA, analysed monthly mean temperature and population data from 24 locations in Saudi Arabia for 1985–2010 and found no link between the temperature increase and population increase. Thus, there is need for more studies on the relationship between regional warming and local (urban) warming in the MENA with a wider region coverage and recent observations.

In this work, a spatially extended and up-to-date investigation of the observed air temperature trends in the MENA region is carried out, based on mean temperature 1981–2020 time-series from more 370 stations in total (268 from GSOD and 108 used in the construction of the CRUTEM4.6 dataset (Osborn and Jones 2014)). We also use the station metadata, in conjunction with urbanisation data, to explore geographical, topographical and urbanisation effects on the calculated temperature trends.

2 Data and Methodology

2.1 Data

2.1.1 Temperature Station Data

We combine monthly mean near-surface air temperature from two global observational datasets. The first are monthly time-series from the weather stations implemented in the Climatic Research Unit Temperature (CRUTEM version 4.6) dataset.[1] The second are daily time-series from the Global Summary of the Day (GSOD) derived from the Integrated Surface Hourly (ISH) dataset (both produced by the National Climatic Data Center (NCDC)).[2]

These "raw" data also include metadata for each station (e.g., station ID, station name, coordinates, elevation, start year of data, end year) that assist the subsequent analysis. We select the stations that lie inside the Mediterranean and MENA region (15.0 ° N to 46.0 ° N and −20.0 ° W to 65.0 ° E) and with records up to the end of 2020. The GSOD daily data are transformed into monthly mean values based on the 5/3 rule following the WMO Guidelines on the Calculation of Climate Normals[3] by accepting only 5 days of missing

[1] https://crudata.uea.ac.uk/cru/data/temperature/crutem4/station-data.htm.

[2] https://www.ncei.noaa.gov/access/metadata/landing-page/bin/iso?id=gov.noaa.ncdc:C00516.

[3] https://library.wmo.int/doc_num.php?explnum_id=4166.

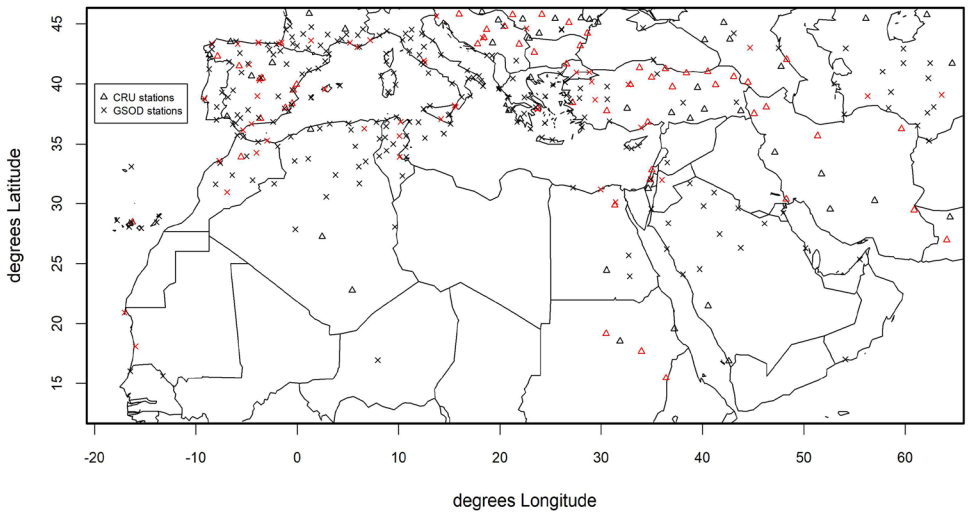

Fig. 1 Distribution of temperature stations in the MENA study domain (triangles for CRUTEM, "x" for GSOD). The urban centre class stations (according to 2.2.2) are distinguished with red colour

observations per month and not more than 3 consecutive missing days. From the resulting monthly time-series, we obtain 268 GSOD and 102 CRUTEM stations with missing values less than the 10% of the data, thus providing a 370 station combined dataset with a fairly representative spatial distribution across the region, as shown in Fig. 1.

2.1.2 Urbanisation Data

Data from the Global Human Settlement Model (GHS-SMOD) spatial grid are used to represent urbanisation levels in the study region. The GHS-SMOD distinguishes the global built-environment into settlement types (cities, towns and suburbs, and rural areas) based on population density, size and geospatial identification of adjacent grid cells via the Degree of Urbanisation methodology (Dijkstra et al. 2021). This dataset is part of the Global Human Settlement Layer (GHSL) project that is becoming an indispensable tool for quantifying human presence and processes (Ehrlich et al. 2021). The assumptions for the settlements classification at the two hierarchical levels L1 and L2 for GHS-SMOD are detailed in section 2.4 of the Joint Research Centre (JCR) Technical Report (Freire et al. 2019). In 2.2.2, we specify the classes implemented for the urban characterisation of the stations.

2.2 Methodology

2.2.1 Temperature Trend Analysis

For all station monthly time-series (December 1980 to November 2020), linear trends are calculated for each calendar month and their annual and seasonal averages are derived to assess the period 1981–2020. This is achieved by employing the R-Project linear model (lm) function,[4] that performs a linear regression between the response variable (temperature) and the explanatory variable (time in months) (Crawley 2015). For each station time series, we quantify the slope β, corresponding to the magnitude of the temperature trend, and the standard error ϵ. The calculated trends for each calendar month are deemed as statistically significant at the 95% confidence level, if the ratio $\frac{\beta}{\epsilon}$ is greater than 2 (Santer et al. 2000).

For each station, the seasonal average trend (e.g. JJA for June–July–August) is derived by taking the mean of the slope values of the respective 3 months and is considered as statistically significant only when all 3 months are statistically significant according to the $\frac{\beta}{\epsilon}$ greater than 2 criterion. The annual average trend for each station is derived by taking the respective 4-seasons average and is considered as statistically significant only when all 4 seasons are statistically significantly according to the preceding approach. This treatment is relevant for Fig. 3 where trends (with statistical significance indication) for all stations are depicted in maps.

The seasonal and annual trends averaged for many stations (all or of different urbanisation class) used in Tables 1 and 2 and Fig. 6, are derived from one-sample t-tests with the respective monthly slope values. The difference in the monthly trends between the urban centre and the other two urbanisation characterisations used in Fig. 7 is derived from two-sample t-tests. These procedures also provide the confidence intervals at the 95% level.[5]

[4] https://www.rdocumentation.org/packages/stats/versions/3.6.2/topics/lm.

[5] https://www.rdocumentation.org/packages/stats/versions/3.6.2/topics/t.test.

2.2.2 Urban Characterisation

The degree of urbanisation of the MENA stations is determined by assigning to them three classes (L1 nomenclature) from (further aggregating) the Global Human Settlement Model layer (GHSL-SMOD) data for the year 2000 as follows (in parenthesis the settlement classes considered from the L2 GHSL-SMOD grids):

- "Urban Centre" (urban centre);
- "Urban Cluster" (dense urban, semi-dense urban, suburban and peri-urban clusters);
- "Rural" (rural, low density rural and very low density rural clusters).

The underlying GHS built-up area and population grids are available for the years 1975, 1990, 2000 and 2014/2015. The urban characterisation is applied based on the data for 2000, which is half-way in the period of the temperature trend analysis (1981–2000) and therefore does not account for any changes with time of the urban class among the stations. Figure 2 shows an example over the south Levant of how the three classes from the GHSL-SMOD layer are utilised to characterise the urbanisation of the weather stations used in the trend analysis. Following this classification, out of the 370 stations in total, 100 are characterised as urban centre (marked with red colour in the Fig. 1 map), 71 as urban cluster and 199 as rural.

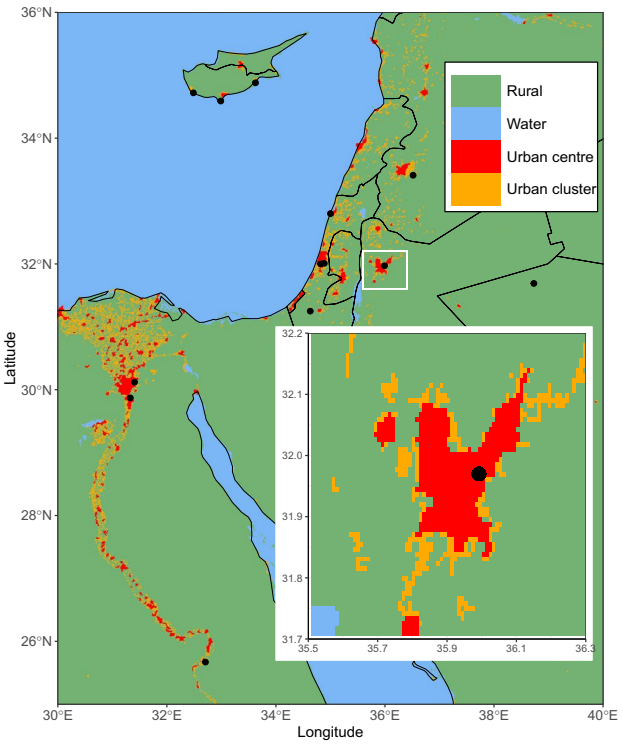

Fig. 2 An example representation of the three classes distinguished by colours (Urban Centre with red, Urban Cluster with orange, Rural with green) based on the GHSL-SMOD layer over the south Levant for the year 2000. Also shown are the locations (black dots) of the meteorological stations used in the trend analysis. The inset map zooms over Jordan, where the indicated station (Marka International Airport) is characterised as urban centre

3 Results

3.1 Seasonal Dependence

Figure 3 shows the annual and summer trends calculated according to 2.2.1 for the period 1981-2020. It is evident that the vast majority of stations exhibit positive trends. Only 24 stations situated in western Mediterranean have negative trends (all non-statistically significant), while the stronger warming occurs over south-East Europe and the Middle East. The negative trends in those few stations has not been reported in previous studies of mean temperature trends in Spain (del Río et al. 2011; Garcia 2015; Moratiel et al. 2017), however these referred to periods up to 2010, and a slowing down of the positive trends over that sub-region has been shown to occur after 2005 (Sandonis et al. 2021). The distribution of the trend for the whole region (Fig. 4) demonstrates the dominance of positive values and reveals their greater occurrence for summer and spring than the rest of the seasons, especially for trends > 0.5 ° C/decade (hence the slightly more platykurtic distribution of the summer values compared to the others).

Table 1 provides a numerical comparison of the trend values averaged annually and for all seasons. Summer (JJA) and spring (MAM) stand out as the faster warming seasons, with trends of 0.45 and 0.43 °C/decade respectively, while winter (DJF) and autumn (SON) exhibit smaller warming (0.27 and 0.30 ° C/decade respectively). These numbers result in an annual trend of 0.36 °C/decade. From the same table, it is also evident that for all seasons at least half of the stations experience trends greater than 0.3°C/decade. The number of stations with event faster warming (> 0.6°C/decade) is also noteworthy, with 109 counts (about 29% of the total) in summer and 80 counts in spring (22% of the total).

3.2 Geographical Dependence

Figure 5 explores the association between the annual trends and the stations' main geographical characteristics. The most pronounced, and linear, relationship (correlation coefficient r ∼ 0.5) appears to hold between the annual trend and the longitude (also discernible in Fig. 3), confirming the occurrence of stronger warming rates eastwards. A per month calculation (not shown) separately for the stations

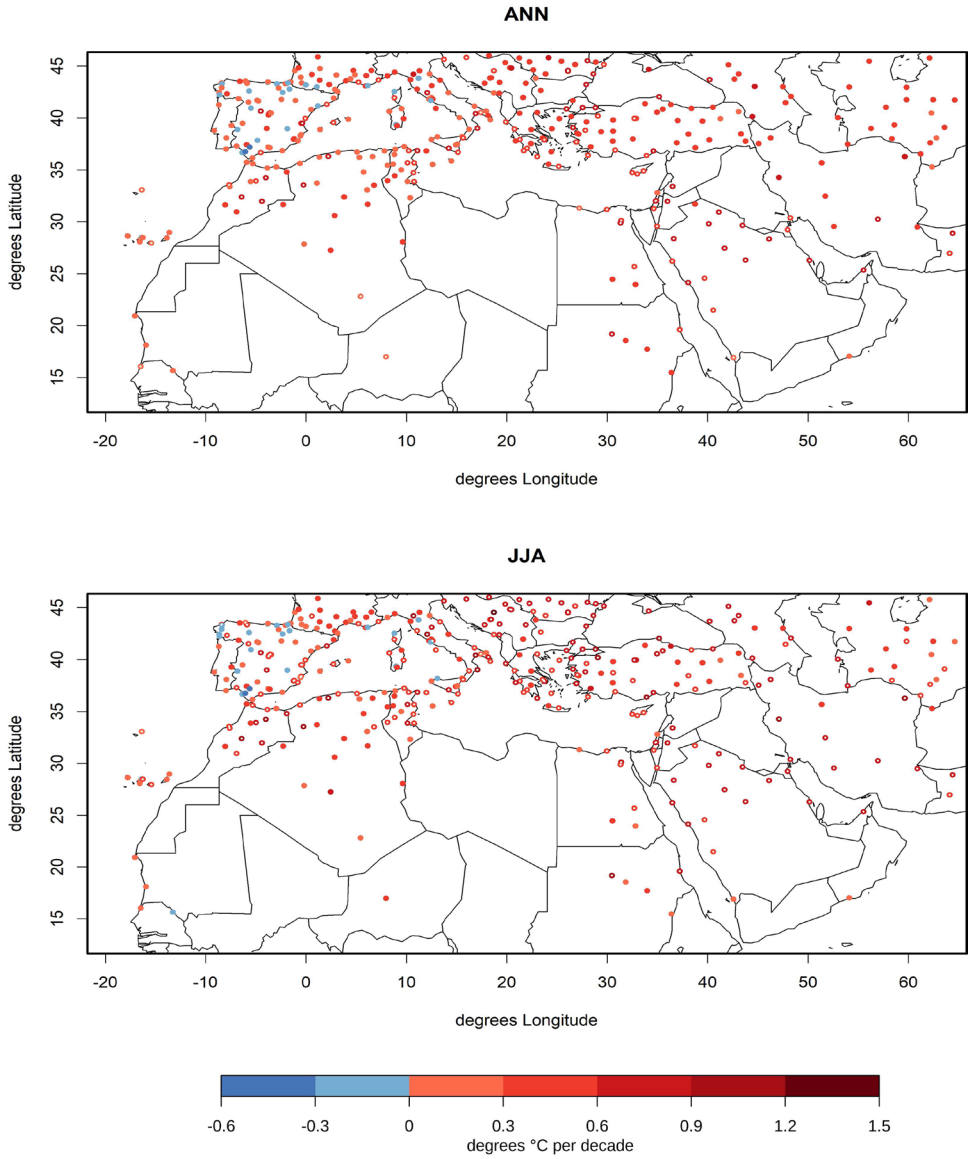

Fig. 3 Annual (up) and summer (down) 1981–2020 trends in ° C/decade for CRUTEM and GSOD stations. The filled circles with the white dots represent statistical significance at the 95% confidence level

east and west of 20 °E, reveals that the trend for the 159 eastern stations is larger than the trend of the 211 western stations for 10 out of the 12 calendar months (by about 0.5°C /decade for February and March and 0.2 − 0.3°C/decade for June–August). A reverse, but less marked relationship (r ∼ 0.4) is seen between the trend and the latitude, indicating weaker warming from the southern towards the northern parts of the MENA domain.

Smaller positive and generally linear correlations of the trend against altitude and distance from sea are derived (respectively, with r ∼ 0.1 and ∼ 0.2). These are valid for the stations that are not in low elevation (altitude > 0.5 km) or near the coast (distance from sea > 100 km) and point to a small tendency in the warming rate to be larger the higher above the ground and the further away from the sea the measurement station is. Note that these two factors are co-correlated (r ∼ 0.4) due to the topography (mountains exist further inland). The small positive correlation between the annual trend and elevation, corroborates the elevation-dependent warming observed in other regions (but not confirmed when pooling together all mountain/lowland studies globally) as reviewed by Pepin et al. (2022). As for the influence of the sea, if a threshold of 100 km is applied (Miller et al. 2003), it is derived (not shown) that the annual and all seasonal trends of the 148 inland stations (distance from sea > 100 km) are larger than the respective trends of the 222 coastal stations (distance from sea <= 100 km). This implies a dampening effect of the Mediterranean Sea on the positive air temperature trends of the nearby stations, despite the increasing warming of the sea surface temperatures in the same period (Pastor et al. 2020).

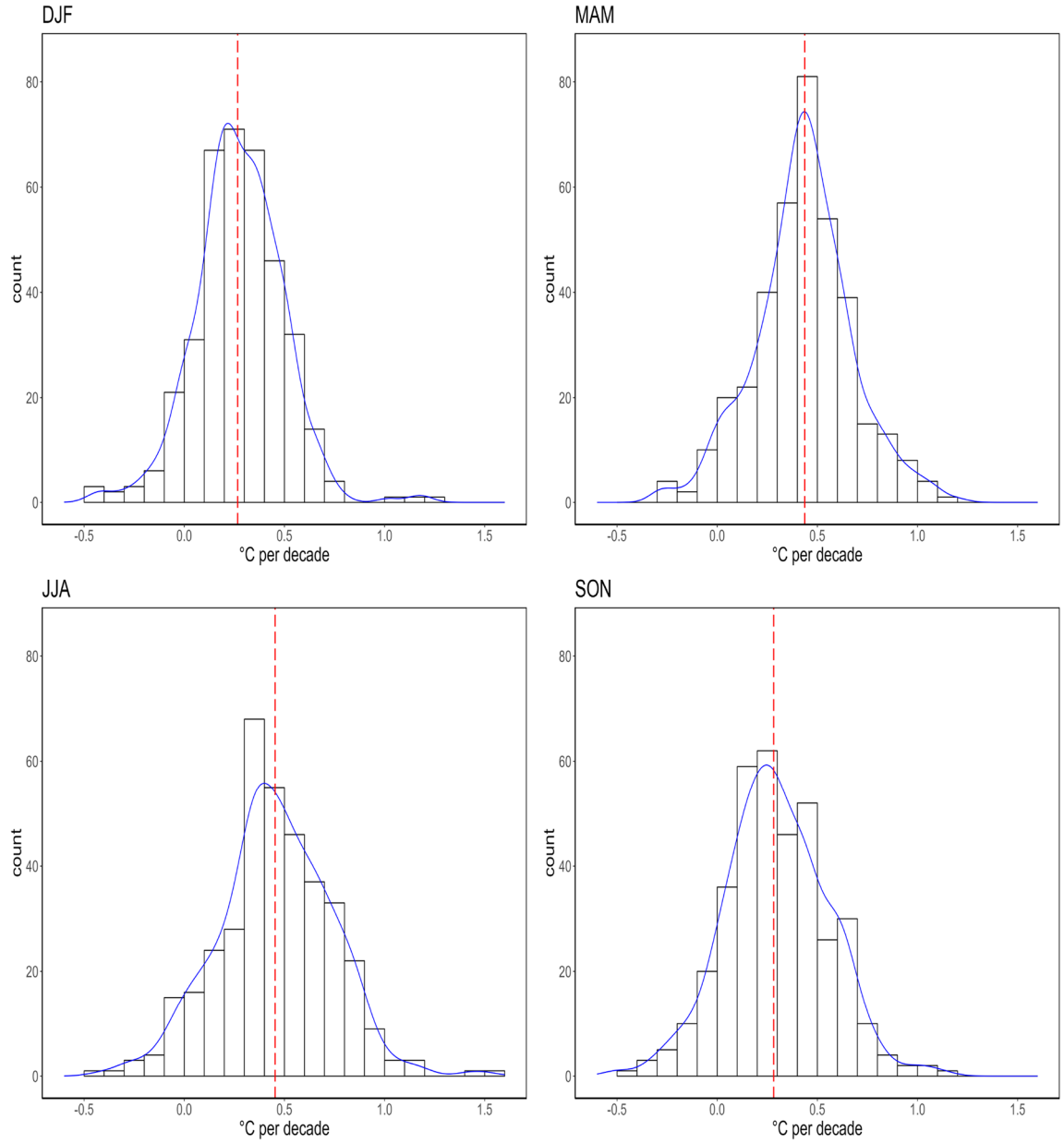

Fig. 4 Distribution (counts histogram with blue density curve) per season of 1981–2020 all station trends in ° C/decade. The vertical dashed red lines define the median value for each season

3.3 Effect of Urbanisation

We next assess the derived temperature trends according to the urban characterisation of the stations, following 2.2.2. Table 2 lists the magnitude of the annual and seasonal trends averaged for all stations as well for the three classes (urban centre, urban cluster and rural) as calculated with one-sample t-tests described in 2.2.1. Figure 6 depicts the same information as Table 2 and visually assists the following interpretation.

The seasonal and annual average trends derived from the urban centre stations are larger than the ones derived from all MENA stations. The annual trend from the urban centre stations is 0.43 °C/decade, 19% greater than that for all stations (0.36 °C/decade). Seasonally, the urban centre warming rates are greater than those from all stations during summer in absolute terms (i.e. 0.54 °C/decade vs 0.45 °C/decade, or by 20%) and during autumn in relative terms (i.e. 0.39 °C/decade vs 0.30 °C/decade, or by 30%). The trends (annual and seasonal) derived from the rural stations are

Table 1 Annually and seasonally averaged 1981–2020 trends averaged for all MENA stations (all values are statistically significant at the 95% level)

Season	All stations $°C/decade$	No. stations $> 0.3°C/decade$	No.stations $> 0.6°C/decade$
ANN	0.36 ± 0.009	236	55
DJF	0.27 ± 0.017	166	21
MAM	0.43 ± 0.019	272	80
JJA	0.45 ± 0.018	278	109
SON	0.30 ± 0.019	173	49

Also, number of stations with trends greater than 0.3°C/decade and 0.6°C/decade

smaller than those from urban centre and this finding alone suggests a different temporal behaviour of the observed air temperature for the two classes. However, the trends derived from the rural stations are, within the 95% confidence intervals (Table 2), almost the same with those from all stations, implying a negligible influence of the urban centre stations in the overall trend. Another observation from Table 2 is that the trends from the urban cluster stations are smaller than, not only the city centre, but also the rural ones. In order to further investigate this, would require locally and temporally detailed information (e.g. time-dependent land cover and use) in order to explore magnitudes and rates of change of green and impervious areas in the suburbs versus the other urban classes.

Figure 7 quantifies the monthly variation of the difference between the trend derived from the 100 urban centre stations only and the trend from the 270 stations comprising urban cluster and rural classes. The mean values per month and the respective confidence intervals and statistical significance at the 95% level are calculated with a two-sample t-test for the monthly trend data of the two groups of stations. For all calendar months (except April, May and December) the difference in the trend is statistically significant, with values between 0.05 and 0.15 °C/decade, greater for summer and autumn, and an annually mean of 0.097 ± 0.023 °C/decade. This difference, indicative of a slightly faster rate of warming in the urban centre stations compared to the rest, is small in absolute terms

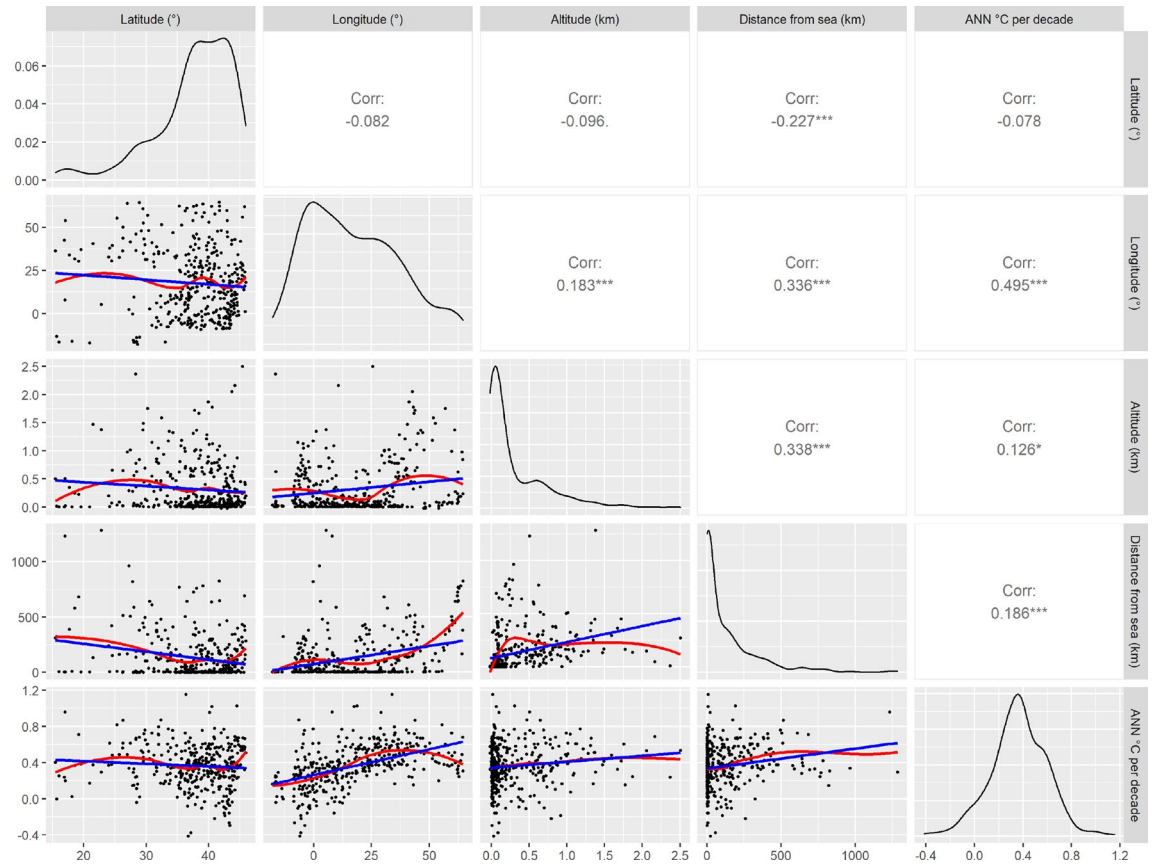

Fig. 5 Pairs plot of annual trends (ANN, °C/decade) latitude & longitude (in °), and altitude & distance from the sea (in km). The diagonal (from top left to bottom right) consists of the densities of the variables and the numbered panels show the correlation coefficients between the variables (corresponding to the far most scatterplot moving diagonally left). The red curves and blue lines are the loess and linear fits, respectively

Table 2 Annual and seasonal temperature trends for the whole station sample ("All") and subsets of stations according to urban characterisation ("urban centre", "urban cluster" and "rural class")

Trend ° C/decade						
	ANN	DJF	MAM	JJA	SON	*n*
All	0.36±0.009	0.27±0.017	0.43±0.019	0.45±0.018	0.30±0.019	370
Urban centre	0.43±0.018	0.33±0.036	0.48±0.018	0.54±0.032	0.39±0.037	100
Urban cluster	0.31±0.020	0.22±0.035	0.37±0.041	0.40±0.039	0.24±0.040	71
Rural	0.35±0.013	0.26±0.022	0.43±0.026	0.43±0.025	0.27±0.025	199

All values are statistically significant at the at the 95% level. *n* = sample size

and equivalent to an additional average warming of about 0.4 °C/decade during 1981–2020.

4 Summary and Conclusions

The observed tendency in near surface air mean temperature over the MENA region during the last four decades has been assessed by utilising monthly time series from 370 weather stations included in the GSOD and CRU datasets. These point measurements allow the calculation of trends in a spatially precise manner, free of the corrections and area smoothing applied in derivative, gridded climate datasets.

Following linear trend calculations, strong warming rates have been derived for the period 1981–2020. The MENA domain average annual trend is about 0.4 °C/decade, twice as large as the global average, and in agreement with other studies that include recent data up to the end of the last decade (Odnoletkova and Patzek 2021). The warming is a little faster during summer and spring (approaching 0.5 ° C/decade) and somewhat slower during winter and autumn (< 0.3 °C/decade). A pronounced longitudinal gradient was derived, where the locations eastern of 20 °E seem to have warmed faster than the western ones, adding to the conclusion of a recent assessment that the eastern Mediterranean and the Middle East (EMME) is a prominent climate change hotspot within MENA and globally (Zittis et al. 2022).

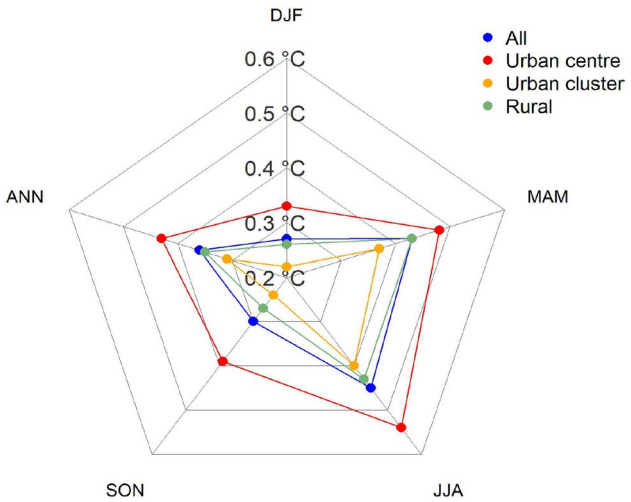

Fig. 6 Radar chart of annual and seasonal temperature trends for the whole station sample ("All") and subsets of stations according to urban characterisation ("urban centre", "urban cluster" and "rural class")

This sub-regional preference of the accelerated warming, especially for the summer period, could be the result of the influence of several atmospheric and surface drivers. The climate change-induced winter/spring rainfall decrease in EMME (Zittis 2018) enhances warming in the following summer season through soil moisture–air temperature interaction over the areas sensitive to this effect (Zittis et al. 2014). The operation of this link has contributed to the observed increase in atmospheric aerosol loading in the Middle East, related to soil drying and elevated mineral dust emissions (Klingmüller et al. 2016). At places, the arid surface of MENA also favours enhanced warming through the desert amplification effect due to higher downward long-wave radiation forcing from the warmer and, thus, more moist atmosphere (Zhou 2016). Atmospheric tele-connections may also contribute to the increasing summer-time air temperatures in the Middle East, brought about by circulation changes involving ocean–atmosphere interactions from the North Atlantic to the Indian Ocean and the Arabian Sea (Xoplaki et al. 2003; Skliris et al. 2012; Almazroui and Hasanean 2020; Ehsan et al. 2020).

By grouping the stations according to the GHS-SMOD spatial grid which assigns a degree of urbanisation, we analysed the calculated trends for urban centre, urban cluster and rural classes. We found that the urban centre stations exhibited larger trends compared to all stations or the urban cluster and rural ones, especially for summer (about 0.5 ° C/decade vs 0.4 °C/decade). The annual average difference was a statistically significant 0.1 °C/decade, revealing an urbanisation signature in the derived trends. This result is quantitatively similar to those in studies for other regions and using different methods to disentangle the effect of

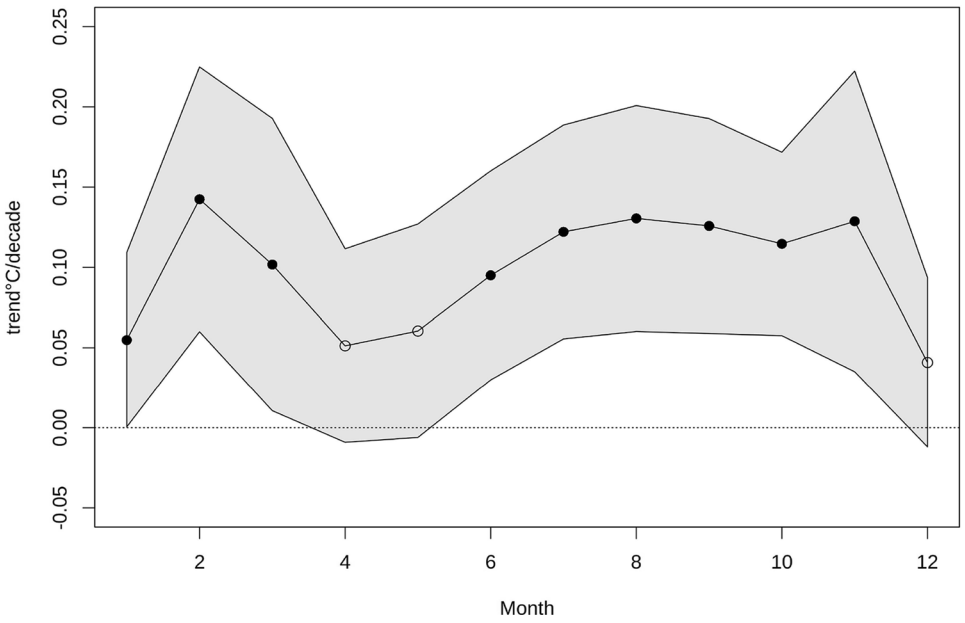

Fig. 7 Difference of 1981–2020 trend (°C/decade) for every calendar month between the stations characterised as urban centre against those as urban cluster plus rural. The shaded area represents the range defined from the higher and lower confidence intervals of the difference. Solid (open) circles denote presence (absence) of statistical significance at the 95% level

surface processes and urbanisation on observed air temperature trends (Kalnay et al. 2006; Sun et al. 2016). However, much smaller urbanisation contribution to daily mean temperature trends has also been derived, for example, an annual 0.003 °C/decade and summer 0.01 °C/decade over Europe for 1990–2006 based on ECAD weather station and CORINE land use data (Chrysanthou et al. 2014).

Our results, based on mean temperature monthly data, show that urban centre areas have warmed slightly faster than rural ones in the last four decades, but the urbanisation contribution to the overall strong warming in the MENA region is small. Further work could involve trend analysis of maximum and minimum temperature, from a higher number of stations and additional sources. This would allow a detailed consideration of urban heat island effects that operate in diurnal time scales.

Funding Open Access funding enabled and organized by Projekt DEAL. This work was co-funded by the European Regional Development Fund and the Republic of Cyprus through the Research Innovation Foundation CELSIUS Project EXCELLENCE/1216/0039. It was also supported by the EMMECARE project that has received funding from the European Union's Horizon 2020 Research and Innovation Programme, under grant agreement no. 856612, as well as matching co-funding by the Government of the Republic of Cyprus.

Declarations

Conflict of interest The Authors declare no conflict of interest.

References

Almazroui M (2019) Temperature changes over the CORDEX-MENA domain in the 21st Century using CMIP5 data downscaled with RegCM4: a focus on the Arabian Peninsula. Adv Meteorol. https://doi.org/10.1155/2019/5395676

Almazroui M (2020) Summer maximum temperature over the gulf cooperation council states in the twenty-first century: multimodel simulations overview. Arab J Geosci. https://doi.org/10.1007/s12517-020-05537-x

Almazroui M, Hasanean HM (2020) Saudi Arabia's summer surface air temperature and its association with circulation patterns. Int J Climatol 40(13):5727–5743. https://doi.org/10.1002/joc.6547

Almazroui M, Hasanean HM, Al-Khalaf AK, Basset HA (2013) Detecting climate change signals in Saudi Arabia using mean annual surface air temperatures. Theoret Appl Clmatol 113(3–4):585–598. https://doi.org/10.1007/s00704-012-0812-x

Almazroui M, Islam MN, Jones PD (2013) Urbanization effects on the air temperature rise in Saudi Arabia. Climatic Change 120(1–2):109–122. https://doi.org/10.1007/s10584-013-0796-2

Brohan P, Kennedy JJ, Harris I, Tett SF, Jones PD (2006) Uncertainty estimates in regional and global observed temperature changes: a new data set from 1850. J Geophys Res Atmos. https://doi.org/10.1029/2005JD006548

Chrysanthou A, Schrier GVD, Besselaar EJVD, Tank AMK, Brandsma T (2014) The effects of urbanization on the rise of the european temperature Since 1960. Geophys Res Lett 41:7716–7722. https://doi.org/10.1002/2014GL061154

Crawley MJ (2015) Statistics : An introduction Using R, 2nd Edition. John Wiley & Sons, Ltd

del Río S, Herrero L, Pinto-Gomes C, Penas A (2011) Spatial analysis of mean temperature trends in spain over the period 1961–2006.

Global Planet Change 78:65–75. https://doi.org/10.1016/j.gloplacha.2011.05.012
Dijkstra L, Florczyk AJ, Freire S, Kemper T, Melchiorri M, Pesaresi M, Schiavina M (2021) Applying the degree of urbanisation to the globe: a new harmonised definition reveals a different picture of global urbanisation. J Urban Econ 125:103312. https://doi.org/10.1016/J.JUE.2020.103312
Doblas-Reyes F, Sörensson A, Almazroui M, Dosio A, Gutowski W, Haarsma R, Hamdi R, Hewitson B, Kwon WT, Lamptey B, Maraun D, Stephenson T, Takayabu I, Terray L, Turner A, Zuo Z (2021) Linking global to regional climate change, Cambridge University Press, Cambridge, United Kingdom and New York, NY, USA, p 1363-1512. https://doi.org/10.1017/9781009157896.012
Driouech F, ElRhaz K, Moufouma-Okia W, Arjdal K, Balhane S (2020) Assessing future changes of climate extreme events in the CORDEX-MENA region using regional climate model ALADIN-climate. Earth Syst Environ 4(3):477–492. https://doi.org/10.1007/s41748-020-00169-3
Ehrlich D, Freire S, Melchiorri M, Kemper T (2021) Open and consistent geospatial data on population density, built-up and settlements to analyse human presence, societal impact and sustainability: a review of GHSL applications. Sustainability. https://doi.org/10.3390/su13147851
Ehsan MA, Nicolì D, Kucharski F, Almazroui M, Tippett MK, Bellucci A, Ruggieri P, Kang IS (2020) Atlantic Ocean influence on Middle East summer surface air temperature. NPJ Climate Atmos Sci 3(1):1–8. https://doi.org/10.1038/s41612-020-0109-1
Freire S, Corbane C, Zanchetta L, Schiavina M, Politis P, Kemper T, Ehrlich D, Pesaresi M, Maffenini L, Florczyk A, Melchiorri M, Sabo F (2019) GHSL data package 2019: Joint Research Centre (JRC) public release GHS P. Publications Office of the European Union, doi/. https://doi.org/10.2760/290498
Garcia MJL (2015) Recent warming in the balearic sea and spanish mediterranean coast, towards an earlier and longer summer. Atmósfera 28:149–160
Gulev S, Thorne P, Ahn J, Dentener F, Domingues C, Gerland S, Gong D, Kaufman D, Nnamchi H, Quaas J, Rivera J, Sathyendranath S, Smith S, Trewin B, von Schuckmann K, Vose R (2021) 2021: Changing State of the Climate System, Cambridge University Press, Cambridge, United Kingdom and New York, NY, USA, p 1363-1512. https://doi.org/10.1017/9781009157896.004
Hansen J, Ruedy R, Sato M, Lo K (2010) Global surface temperature change. Rev Geophys 48(4):1–29. https://doi.org/10.1029/2010RG000345
He Y, Jia G, Hu Y, Zhou Z (2013) Detecting urban warming signals in climate records. Adv Atmos Sci 30(4):1143–1153. https://doi.org/10.1007/s00376-012-2135-3
Jones P (2016) The reliability of global and hemispheric surface temperature records. Adv Atmos Sci 33(3):269–282. https://doi.org/10.1007/s00376-015-5194-4
Jones PD, Lister DH, Li Q (2008) Urbanization effects in large-scale temperature records, with an emphasis on China. J Geophys Res Atmos 113(16):1–12. https://doi.org/10.1029/2008JD009916
Jones PD, Lister DH, Osborn TJ, Harpham C, Salmon M, Morice CP (2012) Hemispheric and large-scale land-surface air temperature variations: an extensive revision and an update to 2010. J Geophys Res Atmos. https://doi.org/10.1029/2011JD017139
Kalnay E, Cai M, Li H, Tobin J (2006) Estimation of the impact of land-surface forcings on temperature trends in eastern united states. J Geophys Res Atmos. https://doi.org/10.1029/2005JD006555
Klingmüller K, Pozzer A, Metzger S, Stenchikov GL, Lelieveld J (2016) Aerosol optical depth trend over the Middle East. Atmos Chem Phys 16:5063–5073. https://doi.org/10.5194/acp-16-5063-2016
Lelieveld J, Hadjinicolaou P, Kostopoulou E, Chenoweth J, El Maayar M, Giannakopoulos C, Hannides C, Lange M, Tanarhte M, Tyrlis E, Xoplaki E (2012) Climate change and impacts in the Eastern Mediterranean and the Middle East. Climatic Change. https://doi.org/10.1007/s10584-012-0418-4
Lelieveld J, Proestos Y, Hadjinicolaou P, Tanarhte M, Tyrlis E, Zittis G (2016) Strongly increasing heat extremes in the Middle East and North Africa (MENA) in the 21st century. Climatic Change. https://doi.org/10.1007/s10584-016-1665-6
Mckee M, Keulertz M, Habibi N, Mulligan M, Woertz E (2017) Demographic and economic material factors in the MENA region. Middle East and North Africa Regional Architecture: Mapping Geopolitical Shifts, Regional Order and Domestic Transformations (3):1–43, http://www.menaraproject.eu/wp-content/uploads/2017/10/menara_wp_3.pdf
Miller ST, Keim BD, Talbot RW, Mao H (2003) Sea breeze: structure, forecasting, and impacts. Rev Geophys. https://doi.org/10.1029/2003RG000124
Moratiel R, Soriano B, Centeno A, Spano D, Snyder RL (2017) Wet-bulb, dew point, and air temperature trends in spain. Theoret Appl Climatol 130:419–434. https://doi.org/10.1007/s00704-016-1891-x
Morice CP, Kennedy JJ, Rayner NA, Jones PD (2012) Quantifying uncertainties in global and regional temperature change using an ensemble of observational estimates: The HadCRUT4 data set. J Geophys Res Atmos 117(8):1–22. https://doi.org/10.1029/2011JD017187
Ntoumos A, Hadjinicolaou P, Zittis G, Lelieveld J (2020) Updated Assessment of temperature extremes over the Middle East-North Africa (MENA) Region from oservational and CMIP5 data. Atmosphere 11(8):813. https://doi.org/10.3390/atmos11080813
Odnoletkova N, Patzek TW (2021) Data-driven analysis of climate change in Saudi Arabia: Trends in temperature extremes and human comfort indicators. J Appl Meteorol Climatol 60:1055–1070. https://doi.org/10.1175/JAMC-D-20-0273.1
Oke TR (1982) The energetic basis of the urban heat island. Quarterly J Royal Meteorol Soc 108(455):1–24. https://doi.org/10.1002/qj.49710845502
Osborn TJ, Jones PD (2014) The CRUTEM4 land-surface air temperature data set: construction, previous versions and dissemination via Google earth. Earth Syst Sci Data 6(1):61–68. https://doi.org/10.5194/essd-6-61-2014
Osborn TJ, Jones PD, Lister DH, Morice CP, Simpson IR, Harris IC (2020) Land surface air temperature variations across the globe updated to 2019: the CRUTEM5 dataset. J Geophys Res First published: 15 December 2020, https://doi.org/10.1029/2019JD032352
Pastor F, Valiente JA, Khodayar S (2020) A warming mediterranean: 38 years of increasing sea surface temperature. Remote Sensing 12:1–16. https://doi.org/10.3390/RS12172687
Pepin NC, Arnone E, Gobiet A, Haslinger K, Kotlarski S, Notarnicola C, Palazzi E, Seibert P, Serafin S, Schöner W, Terzago S, Thornton JM, Vuille M, Adler C (2022) Climate changes and their elevational patterns in the mountains of the world. Rev Phys. https://doi.org/10.1029/2020RG000730
Rohde R, Muller RA, Jacobsen R, Muller E, Wickham C (2013) A new estimate of the average earth surface land temperature spanning 1753 to 2011. Geoinform Geostat Overview 01(01):1–7. https://doi.org/10.4172/2327-4581.1000101
Sandonis L, González-Hidalgo JC, PenãAngulo D, Begueriá S (2021) Mean temperature evolution on the spanish mainland 1916–2015. Climate Res 82:177–189. https://doi.org/10.3354/CR01627
Santer BD, Wigley TM, Boyle JS, Gaffen DJ, Hnilo JJ, Nychka D, Parker DE, Taylor KE (2000) Statistical significance of trends and trend differences in layer-average atmospheric temperature time series. J Geophys Res Atmos 105(D6):7337–7356. https://doi.org/10.1029/1999JD901105

Simmons AJ, Berrisford P, Dee DP, Hersbach H, Hirahara S, Thépaut JN (2017) A reassessment of temperature variations and trends from global reanalyses and monthly surface climatological datasets. Quarterly J the Royal Meteorol Soc 143(702):101–119. https://doi.org/10.1002/qj.2949

Skliris N, Sofianos S, Gkanasos A, Mantziafou A, Vervatis V, Axaopoulos P, Lascaratos A (2012) Decadal scale variability of sea surface temperature in the Mediterranean sea in relation to atmospheric variability. Ocean Dynam 62:13–30. https://doi.org/10.1007/s10236-011-0493-5

Sun Y, Zhang X, Ren G, Zwiers FW, Hu T (2016) Contribution of Urbanization to warming in China. Nature Climate Change 6(7):706–709. https://doi.org/10.1038/nclimate2956

Tanarhte M, Hadjinicolaou P, Lelieveld J (2012) Intercomparison of temperature and precipitation data sets based on observations in the Mediterranean and the Middle East. J Geophys Res Atmos. https://doi.org/10.1029/2011JD017293

Wang F, Ge Q, Wang S, Li Q, Jones PD (2015) A new estimation of urbanization's contribution to the warming trend in China. J Climate 28(22):8923–8938. https://doi.org/10.1175/JCLI-D-14-00427.1

Wang J, Yan ZW (2016) Urbanization-related warming in local temperature records: a review. Atmos Ocean Sci Lett 9(2):129–138. https://doi.org/10.1080/16742834.2016.1141658

Xoplaki E, González-Rouco JF, Luterbacher J, Wanner H (2003) Mediterranean summer air temperature variability and its connection to the large-scale atmospheric circulation and ssts. Climate Dynam 20:723–739. https://doi.org/10.1007/s00382-003-0304-x

Yun X, Huang B, Cheng J, Xu W, Qiao S, Li Q (2019) A new merge of global surface temperature datasets since the start of the 20th century. Earth Syst Sci Data 11(4):1629–1643. https://doi.org/10.5194/essd-11-1629-2019

Zhou L (2016) Desert amplification in a warming climate. Scient Rep 6:1–13. https://doi.org/10.1038/srep31065

Zittis G (2018) Observed rainfall trends and precipitation uncertainty in the vicinity of the Mediterranean, Middle East and North Africa. Theoret Appl Climatol 134(3–4):1207–1230. https://doi.org/10.1007/s00704-017-2333-0

Zittis G, Hadjinicolaou P (2017) The effect of radiation parameterization schemes on surface temperature in regional climate simulations over the mena-cordex domain. Int J Climatol 37:3847–3862. https://doi.org/10.1002/joc.4959

Zittis G, Hadjinicolaou P, Lelieveld J (2014) Role of soil moisture in the amplification of climate warming in the eastern mediterranean and the Middle East. Climate Res 59:27–37. https://doi.org/10.3354/cr01205

Zittis G, Hadjinicolaou P, Klangidou M, Proestos Y, Lelieveld J (2019) A multi-model, multi-scenario, and multi-domain analysis of regional climate projections for the Mediterranean. Reg Environ Chang 19(8):2621–2635. https://doi.org/10.1007/s10113-019-01565-w

Zittis G, Almazroui M, Alpert P, Ciais P, Cramer W, Dahdal Y, Fnais M, Francis D, Hadjinicolaou P, Howari F, Jrrar A, Kaskaoutis DG, Kulmala M, Lazoglou G, Mihalopoulos N, Lin X, Rudich Y, Sciare J, Stenchikov G, Xoplaki E, Lelieveld J (2022) Climate change and weather extremes in the eastern mediterranean and Middle East. Rev Geophys. https://doi.org/10.1029/2021RG000762